

A Novel Large-flow-rate Gas Fuel Injection Device with Sensorless Control

Cao Tan, Wenqing Ge, Bo Li, and Binbin Sun

Abstract—Gas fuel injection device (GFID) has a great influence on the performance of compressed natural gas engine. A novel large-flow-rate GFID with simplified sensorless control strategy was proposed in this paper, which adopts a moving-coil electromagnetic linear actuator as driver, and utilizes a plastic gasket to improve the sealing performance. The actuator's actuating force was maximized and linearized utilizing Halbach magnet array and two sets of coils with opposite current. Meanwhile, a landing control strategy based on energy distribution was presented to eliminate bounce and excessive compression while maintaining fast response. The sensorless landing control strategy was simplified according to the features of the actuator. Position detection was carried out to monitor landing process. PD mode iterative learning control was used to adjust distribution point. The results showed that the landing velocity was decreased by 58.5% under rated condition with the proposed control strategy. The bounce and excessive compression of plastic gasket were eliminated with the transition time of 1.8 ms. Consequently, the fuel injection quantity can be controlled precisely and timely.

Index Terms—: *Electromagnetic linear actuator, gas fuel injection device, dynamic performance, sensorless control*

I. INTRODUCTION

THE GFID is a key executive device in engine fuel supply system, which has a great influence on fuel injection quantity. The electromagnetic actuator is simpler, more robust, and easier to manufacture than other actuators [1-4]. In order to enhance the quality of air-fuel mixture, GFID based on electromagnetic actuator has become a research hot spot [5].

Currently, the driver of conventional GFID is mostly solenoid. The conventional GFID is small in size and convenient to install in engine [6-7]. However, it is difficult to supply enough gas fuel to each large-bore engine cylinder individually due to the lack of injection flow-rate [8]. More importantly, conventional GFID always results in undesired impact issues such as bounce, noise, vibration, and harshness, which dramatically reduces the durability, reliability and

precision of the injection system [9]. A large-flow-rate GFID without bounce is in demand of market and technology development.

As for on-off landing control, ensuring fast response simultaneously is the major challenge. It is different from the traditional soft-landing control of electromagnetic actuators. Typical soft-landing control algorithms mainly include iterative learning control [10], inverse system method control [11], and sliding mode control, which are mainly functioned to limit the valve landing velocity [12-13]. There have been many researches reported on sensor-based and senseless soft-landing control, while less reported on on-off landing control.

With actuator being used for the purpose of sensing, external transducer and its accessories, such as mechanical layout and cabling, can be saved. This results in considerably reduced system cost and in improved robustness. In reference [14], an electric brake was to reduce the velocity at the end of stroke for circuit breaker, which increased the system volume. In reference [15-17], sensorless methods were proposed to achieve position or velocity detection based on magnetic signal and electric signal. Meanwhile, signal-input methods for position detection have been discussed [18-19]. Sliding mode [20], nonlinear observer, Kalman filters [21], and hysteresis hybrid extended Kalman filter have been proposed for sensorless control [22]. All these methods mentioned above are restricted in many application fields, for instance the harsh working condition of engine. It is worth noting that all these researches focus on impact between metallic materials, while the impact between plastic and metallic material has never been studied.

This paper is organized as follows. In Section 2, a novel large-flow-rate GFID is designed and modeled for position self-sensing. Section 3 proposes a sensorless energy distribution landing control strategy to eliminate bounce and excessive compression while maintaining fast response. The experiment and analysis of GFID with sensorless landing control are presented in Section 4. Conclusion of this work is given in Section 5.

II. DESIGN AND ANALYSIS

A. Conceptual design of GFID

There are already GFID products with mature technology, as shown in Figure 1 a) and b). The conventional GFID based on solenoid is small in size and convenient to install in engine. This paper presents a GFID for large-bore port fuel injection engines. The specifications of engine are listed in Table 1 [8]. The GFID is driven by a high power density moving-coil permanent magnet linear actuator. The schematic diagram of

Manuscript received January 14, 2019; revised May 20, 2019.

Cao Tan is with School of Transportation and Vehicle Engineering, Shandong University of Technology, 255000 Zibo, Shandong, China (e-mail: njusttancao@yeah.net).

Wenqing Ge is with School of Transportation and Vehicle Engineering, Shandong University of Technology, 255000 Zibo, Shandong, China. (corresponding author to provide phone: +86-0533-2789639; fax: +86-0533-2789639; e-mail: gwq@sdut.edu.cn).

Bo Li is with School of Transportation and Vehicle Engineering, Shandong University of Technology, 255000 Zibo, Shandong, China.

Binbin Sun is with School of Transportation and Vehicle Engineering, Shandong University of Technology, 255000 Zibo, Shandong, China.

solenoid and moving-coil permanent magnet linear actuator are shown in Figure 1 c) and d).

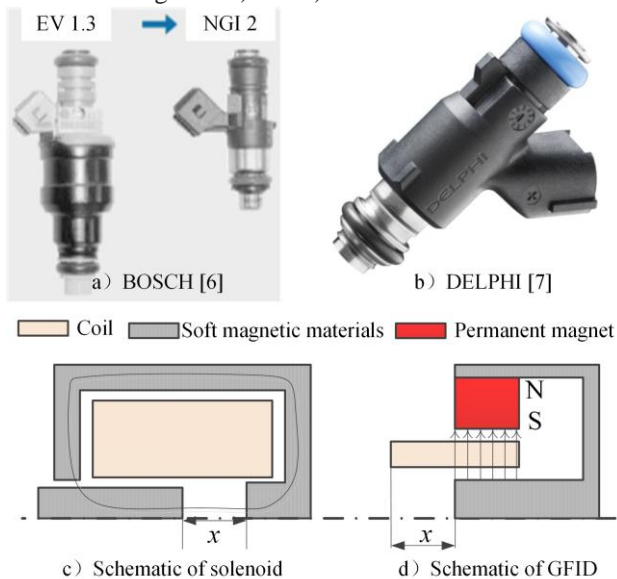


Fig. 1. Existing prototypes and principle comparison of actuators.

TABLE 1. SPECIFICATIONS OF ENGINE

Parameter	Value
Bore ×Stroke (mm)	131×155
Displacement volume (L)	12.53
Compression ratio	11.5
Rated power (kW)/speed (rpm)	255/1900

The GFID mover consists of a gas pipeline, two coils and a plastic gasket, as shown in Figure 2 a). The relative displacement between plastic gasket and valve seat are shown in Figure 2 b). The positive motion direction is regulated as the direction away from valve seat. The compression extreme position is the position where plastic gasket is compressed in the largest design current (i_{max} , driven by 24V DC source u_{max}). The distance from compression initial position to compression extreme position is 0.2 mm. Furthermore, gas fuel injection quantity is controlled precisely by adjusting the open and close phase. The GFID is designed as a poppet valve to operate in pull-open manner. The GFID's characteristics are analyzed as follows.

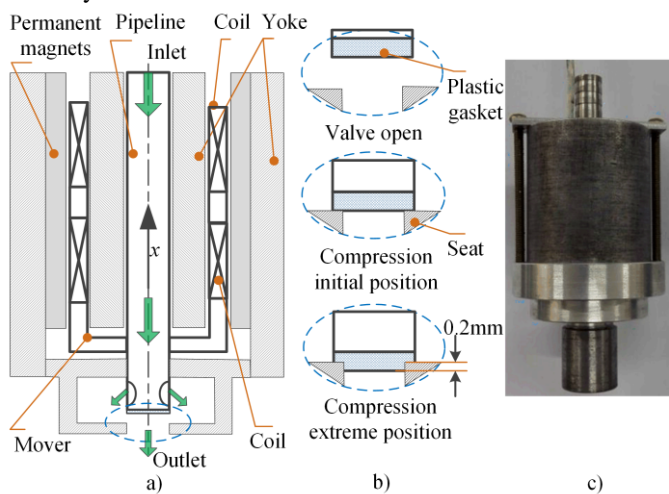


Fig. 2. Schematic and prototype of GFID.

Firstly, A NdFeB permanent magnet is chosen, with remnant

flux density of 1.30 T, coercive force of 990 kA/m and relative permeability of 1.06. Which minimized the energy required and maximized the magnetic flux. Halbach magnet array was utilized to maximize the actuating force by strengthening the magnetic field in the air gap. Figure 3 showed that the flux density in the air gap was enhanced significantly employing Halbach array compared with that without Halbach array. The flux density in air gap versus position for these two cases were shown in Figure 4. The reduction of flux leakage helped to improve the system energy efficiency. The actuator had two sets of coils with opposite current, which can effectively reduce the armature reaction and keep the force sensitivity invariable. The actuating force is independent of position and proportional to current, because the flux density distribution is uniform in work area.

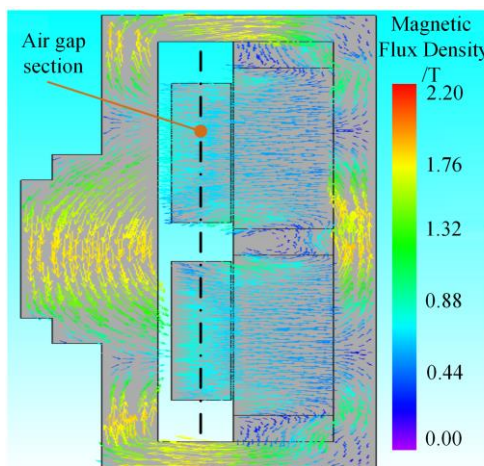


Fig. 3. Magnetic flux density with Halbach array.

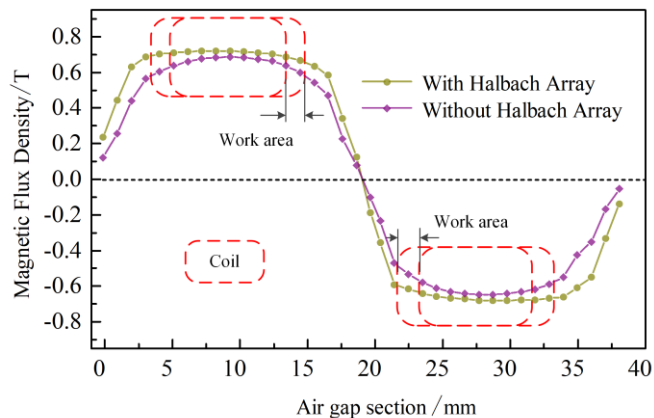


Fig. 4. Magnetic flux density in air gap with or without the Halbach array.

Engineering plastic was applied in valve, with the advantages of qualitative light, sound-absorbing and shock absorption. The application of plastic gasket improved the reliability and the sealing performance. However, the elastic deformation and complex mechanical property in the process of impact brought different challenge to landing control. Because the plastic gasket is a macromolecule polymer material, whose mechanical properties appear to be both nonlinear in constitutive stress-strain relations and strain rate effects in establishing the dynamic constitutive relations [23].

B. GFID prototype

The GFID prototype was shown in Figure 2 c) with the parameters described in Table 2. The electromagnetic force versus current was shown in Figure 5. The experimental setup for force test is given in reference [24]. Where F_m is the Lorentz force, i is the coil current and k_m is the force sensitivity. Simulated and experimental results agreed with each other and the force sensitivity was 11.3 N/A. It is proved that the production of the prototype meets the design requirements. The closing spring was eliminated compared with the conventional GFID, because the actuator has bidirectional output. Moreover, compared with the flat or other linear actuators, the high power density moving-coil permanent magnet linear actuator has the advantages of compact structure, high linearity, high power density and fast response.

TABLE 2. PROTOTYPE PARAMETERS

Parameter	Value
Device height (mm)	70
Device diameter (mm)	35
Outlet diameter (mm)	7
Stroke (mm)	1.25
Motion mass (g)	29
Coil turn count	120
Coil diameter (mm)	0.67
Coil resistance (Ω)	1.89

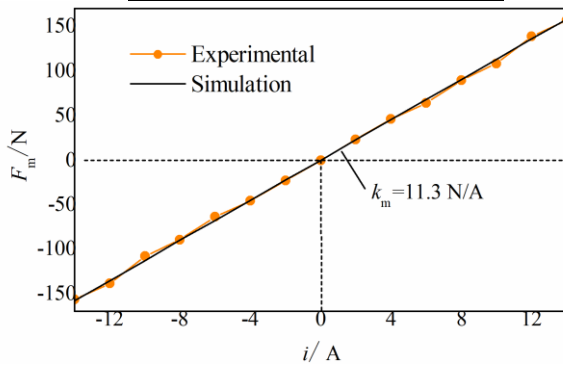


Fig. 5. Variation of electromagnetic force with current.

The characteristic parameters in landing process, based on experimental data, were regulated as Figure 6. In order to close the valve definitely, holding force is needed after valve spool landing. The holding position is defined as the elastic deformation of plastic gasket under holding current. Allowed landing position (valve closing) is defined as the range between the compression initial position and the holding position. The excessive compression is defined as the plastic gasket compressed over the holding position. The bounce is the plastic gasket anti-bounces to move over the compression initial position after compression initial. The transition time (the time in which the plastic gasket moves from 5% of the stroke to the compression initial position) is 1.5ms driven by 24V DC directly. The actuator has the advantage of both fast response and smaller bounce than conventional GFID in reference [8]. However, the serious excessive compression leads to undesired impact issues of noise, vibration, which dramatically reduces the durability, reliability and precision of the GFID system.

Moreover, GFID needs to meet the requirements of gas fuel

injection quantity under any working conditions. The injection duration needs an optimization design constrained in engine speed and load. The gas fuel injection quantity and mixing performance are under researching in our group simultaneously. Thus, fast response of driver is in urgent demand. And the transition time 1.8ms is required to meet the requirements of the gas fuel injection quantity and mixing homogeneity on the rated condition with CA90 injection duration. As a result, eliminating bounce and excessive compression while ensuring fast response simultaneously is the major challenge in GFID landing control. It is different from the traditional soft-landing control of electromagnetic actuators aiming at limiting the valve landing velocity.

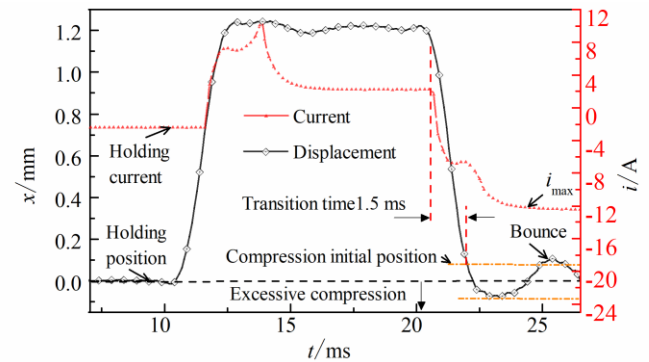


Fig. 6. Characteristic parameters in landing process.

C. Analysis of position detection

The GFID is a coupled electromagnetic-mechanical system [10], and the mathematic model can be described as

$$\begin{cases} \dot{i} = -\frac{R}{L}i - \frac{k_m}{L}v + \frac{u}{L} \\ \dot{x} = v \\ \dot{v} = \frac{F_m}{m} + \frac{F_g}{m} - \frac{N}{m} \end{cases} \quad (1)$$

where R is the resistance, L is the inductance, m is the moving mass, v is the velocity, x is the position of the valve, and u is the voltage applied to the actuator. F_g is the gas force determined by injection pressure. In this paper, F_g is doing positive work to the mover in landing process. The F_m as

$$F_m = k_m i \quad (2)$$

The Lorentz force is proportional to the amount of current. N is the force acting on the plastic gasket when plastic gasket and valve seat is in contact. $N(i, x, v)$ is given by

$$N = \begin{cases} \text{if } x \geq x_i, & 0 \\ \text{if } -0.1 < x \leq x_i, & k_n(x_i - x) \\ \text{if } x = -0.1, & \begin{cases} \text{if } v = 0, & k_m i \\ \text{if } v \neq 0, & \begin{cases} v > 0, & 0 \\ v < 0, & \delta \end{cases} \end{cases} \end{cases} \quad (3)$$

where δ is an impulse function calibrated to give $v^+ = e v^-$, v^+ is the velocity just after impact and v^- is the velocity just before impact. The parameter e , which is less than one, is chosen based on experimental data; -0.1 is the compression extreme position; the parameter k_n stands for the equivalent stiffness coefficient and x_i is the compression initial position.

Additionally, the force sensitivity k_m is kept invariable. The flux density distribution is uniform in coil work area, L is

irrelevant to current (i) and voltage (u). Hence, the position of valve can be detected from equation (1)

$$v(t) = \frac{u(t) - Ri(t) - L \frac{di(t)}{dt}}{k_m} \quad (4)$$

$$x(t) = \int v(t) dt \quad (5)$$

As for the large-flow-rate GFID with plastic gasket driven by high power density moving-coil permanent magnet linear actuator, the impact issue is different from conventional GFID. The position of valve can be detected briefly according to equation (4) and (5), because the force sensitivity k_m is kept invariable. Based on above analysis, a simplified sensorless control was proposed as follow.

III. SENSORLESS LANDING CONTROL

A. Energy distribution control

The landing control of GFID aiming at finding a control law driving the valve spool to the desired position region in a finite transition time without bounce and excessive compression. An energy distribution landing control algorithm was proposed according to the GFID operating characteristics. The main idea behind the approach is to distribute the overall mechanical energy of the GFID mechanical system, defined as

$$E = K + U = \begin{cases} \frac{mv^2}{2} & x \geq x_i \\ \frac{mv^2}{2} + \frac{k_n(x_i - x)^2}{2} & -0.1 < x \leq x_i \end{cases} \quad (6)$$

where K and U are kinetic energy and potential energy respectively. Differentiating (6) and substituting (1), the overall energy rate is simplified as

$$\frac{dE}{dt} = v(F_m - F_g) \quad (7)$$

The above expression confirms that the energy can be directly controlled by meaning of F_m (coil current) being fed to the system. In an ideal situation without energy dissipation, the GFID system is stable and its mechanical and electrical energies are conserved. A soft-landing is achieved when the positive (w_a uses for accelerating) and negative (w_d uses for decelerating) works are equivalent. Thus, the proposed control is to distribute the energy by distributing positive work and negative work done by F_m . The schematic of driving force and anti-force with idea soft-landing control were shown in Figure 7.

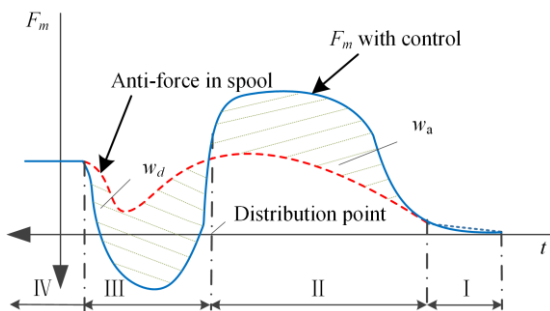


Fig. 7. Schematic of idea landing control.

The complete landing manoeuvre was developed in four different stages as figure 7. In phase I, the electromagnetic field

reserves enough energy to overcome the counterforce, and the armature has not yet started motion. In phase II, the armature is away from the stable position. The armature is accelerating because the F_m is greater than the anti-force. After armature beyond distribution point in phase III, the armature is decelerating because the F_m is smaller than the anti-force. The anti-force will increase again because of compressing plastic gasket when armature reaches the compression initial position. In phase IV, the holding force is equal to the anti-force and armature is stable in allowed landing position. The positive and negative works are distributed by the distribution point, which is the key of the control strategy.

B. Sensorless control strategy

A sensorless landing control method was proposed based on the previous energy distribution control. The control variable can be prompt adjusted in next operating cycle. For this sensorless energy distribution landing control approach, the needed information is extracted from electrical signals such as injector coil voltage and current according to equation (4) and (5) instead of displacement sensor. The diagram of sensorless landing control is shown in Figure 8.

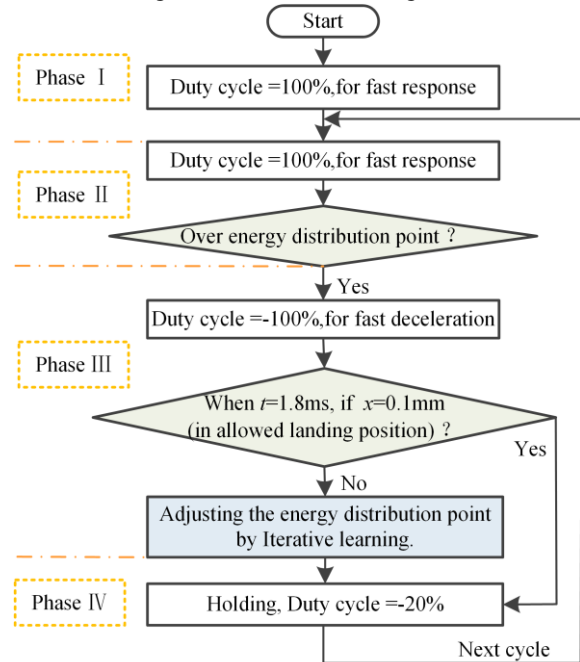


Fig. 8. Sensorless control block diagram of the GFID.

In order to achieve fast response, the duty cycle applying to the coil is 100% in phase I and phase II, while the duty cycle applying to the coil is -100% in phase III. The duty cycle applying to the coil is -20% in phase IV to produce holding current. Hence, the magnitude of the current is governed by the duration. Set the compression initial position ($x=0.1\text{mm}$) as target displacement (x_i) when t is 1.8ms in each cycle. The distribution point is detected from equation (5). The distribution point is adjusted by iterative learning control according to the error of target displacement (e_i). The distribution point in next cycle ($x_{d(N+1)}$) obtain by adjusting the duration of phase II ($t_{d(N+1)}$) from open loop PD mode iterative learning described as

$$t_{d(N+1)} = t_{d(N)} + k_p e_N + k_d \dot{e}_N \quad (8)$$

where N is the number of iterations, k_p is the proportional coefficient and k_d is the differential coefficient. More precision and effective adjusting law for distribution point can be made for researched further. The detection and control of distribution point is the key of the control strategy instead of real-time displacement detection and feedback control. The sensorless landing control method proposed in this paper was simplified. The method adopted distribution point control rather than real-time displacement control, so that the application value was improved.

IV. EXPERIMENT AND ANALYSIS

A. Experimental system and detection verification

The configuration of the experiment system was shown in Figure 9. From the experimental setup, following signals were acquired including the valve spool position (Keyence LK-G85), the coil current (close loop hall-effect current sensor TBC10SY) and the coil voltage (voltage sensor, whose linearity of 0.2%). The fixed-point DSP TMS320F2812 with a clock frequency of 150 MHz was chosen as the digital controller (measurement and control module). The DSP control board, interface circuit, PWM inverter and current sensor were integrated in the controller. The sampling frequency was chosen to be 20 KHz, the switching frequency of PWM inverter was 30 KHz.

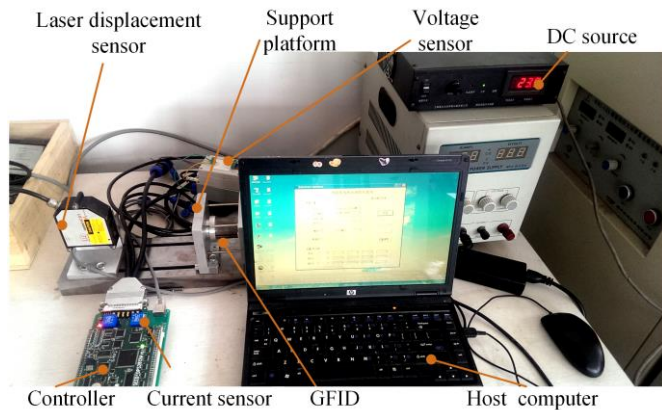


Fig. 9. Experimental setup.

In order to verify the sensorless position detection method of GFID, the experimental (from laser displacement sensor) and detection (from current sensor and voltage sensor) of movement and impact processes under step voltage signal were shown in Figure 10.

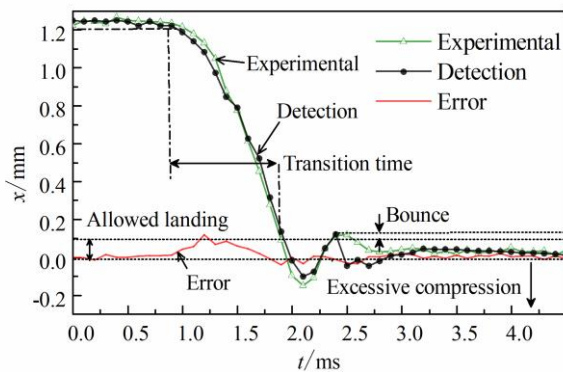


Fig. 10. Comparison of sensor data and detection displacement.

The result of spool displacement between the detection and

experiment were in good agreement within most of the stroke. Hence, the detection can monitor the landing process effectively according to the detection of bounce and excessive compression. The experiment result validated the correctness and precision of the mathematic model and sensorless position detection method of GFID. And all above works give a foundation for landing control.

B. No load analysis

In order to verify the sensorless landing control method based on the energy distribution control, experimental study on continuous 300 cycles was carried out. The results of experimental target displacement and energy distribution point were shown in Figure 11.

The initial energy distribution point was set as the midpoint of stroke (0.6mm), while the experimental position ($t=1.8$ ms) in first cycle was 0.25mm. Which means the GFID didn't close in time. After 8 iterative cycles, the energy distribution point changed from 0.6mm to 0.27mm and kept within specified bounds (0.275 ± 0.025 mm). Meanwhile, the experimental target displacement converged to the target displacement gradually. The control precision of the target displacement was within -0.04 mm. The GFID closed in time and reliable. The results verified that the prototype was stable and the sensorless landing control method was effective. Meanwhile, in order to further study the iterative process, Figure 12 showed the displacement of valve in different iterations.

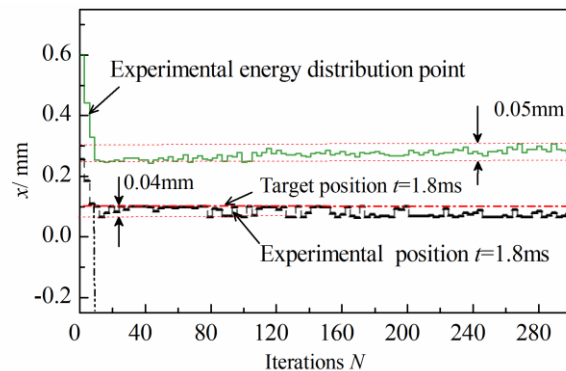


Fig. 11. Experimental iterative convergence process.

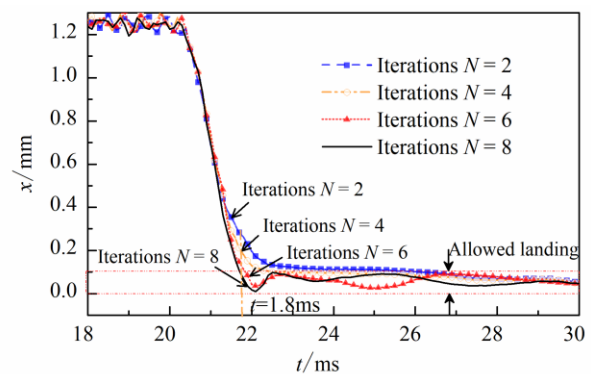


Fig. 12. Experimental landing behavior in different iterations.

The transition time was more than 1.8 ms when energy distribution point larger than 0.3 mm. For fast response, the required energy distribution point was less than 0.3 mm. The energy distribution point was within 0.275 ± 0.025 mm through the iterative learning algorithm. Meanwhile, the compression of plastic gasket was within 0.1 mm so that the excessive

compression was eliminated. The bounce was alleviated compared to traditional GFID. The bounce was also eliminated due to the deceleration produce by the reverse excitation in phase III. Figure 13 showed the specific sensorless control result at the eighth iteration cycle.

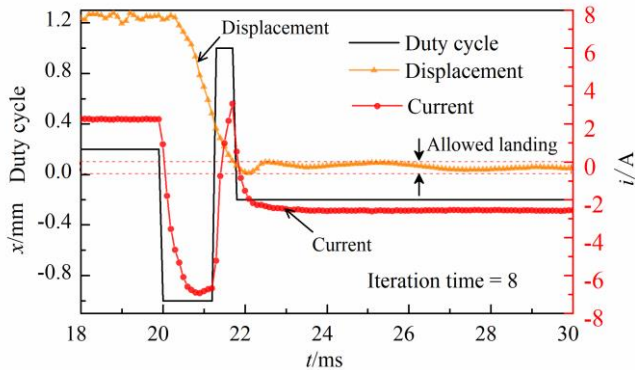


Fig. 13. Experimental result at the eighth iteration cycle.

After the iterative convergence, the experimental result at each iteration cycle was similar with the eighth iteration cycle. Since the error of position detection is objective and the impact between plastic gasket and valve seat is a complex dynamic nonlinear process. The statistical result of landing velocity of 300 iteration cycles was carried out as shown in Figure 14 to evaluate the sensorless landing control method appropriately. The landing velocity with and without the landing control focus on 0.35 ± 0.03 m/s and 0.63 ± 0.03 m/s, respectively. The landing velocity was decreased by 44.4% with sensorless landing control. The undesired impact issues of noise, vibration and harshness was alleviated effectively.

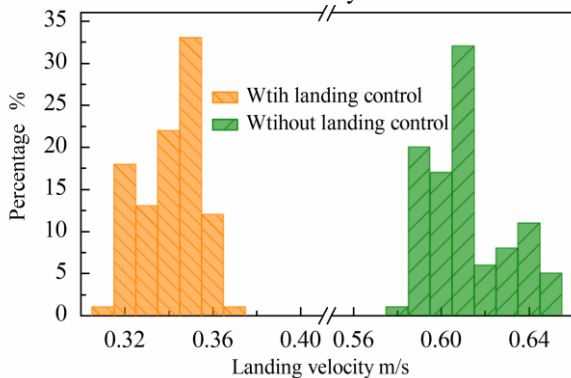


Fig. 14. Statistical result of landing velocity.

Experimental result showed that the valve landed in the desired allowed landing position region, and both of the bounce and excessive compression were eliminated. Moreover, the landing velocity was decreased by 44.4% while the transition time was increased by 20%. Which verified the effectiveness of the sensorless energy distribution landing control strategy.

C. Analysis of landing performance under different injection pressure

To evaluate the novel GFID with sensorless landing control strategy more comprehensively, the dynamic performance of proposed GFID in landing process was simulated under different injection pressure. It was assumed that the injection pressure remained constant during the motion as the mover's motion is within milliseconds. After the iterative convergence, the result was shown in Figure 15.

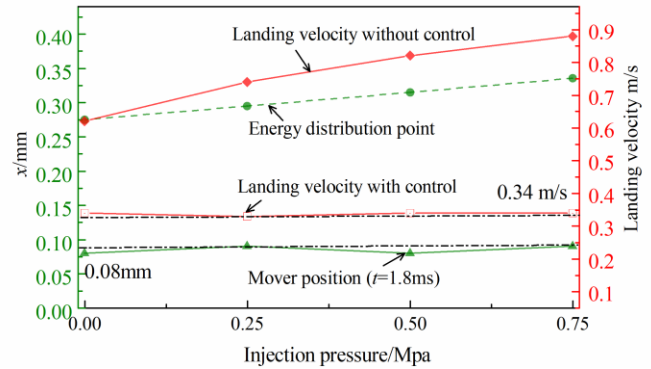


Fig. 15. Dynamic performance in landing process under different injection pressure.

Since the impact between plastic gasket and valve seat was not uncertain in the simulation, the performance parameter in landing process was certain. Without landing control, the transition time was less than 1.5 ms and decreased with the injection pressure, while landing velocity increased with the injection pressure considering the gas force was doing positive work in landing process. Under the sensorless control strategy, the energy distribution point changed from 0.27mm to 0.33mm when the injection pressure changed from 0 Mpa to 0.75 Mpa, while the landing velocity and mover position ($t=1.8$ ms) remained nearby a constant value. Under different injection pressure, landing velocity was decreased by more than 44.4% compared with that without landing control. Under rated condition (injection pressure is 0.5 Mpa), landing velocity was decreased by 58.5%. Moreover, the bounce and excessive compression of the mover (plastic gasket) were eliminated with the transition time of 1.8 ms.

V. CONCLUSIONS

This paper proposes a novel large-flow-rate GFID with sensorless landing control strategy. The characteristic of the novel GFID was analyzed, and the sensorless landing controller was designed and tested. Main results are summarized as followed:

- 1) The actuating force of GFID was maximized and linearized utilizing Halbach magnet array and two sets of coils with opposite current. The invariable force sensitivity and uniform flux density distribution in work area is conducive to fast response and sensorless control.
- 2) The control method was simplified by adopting distribution point control rather than real-time displacement control. The landing velocity was decreased by 58.5% under rated condition with the proposed sensorless landing control strategy. Meanwhile, the bounce and excessive compression were eliminated with the transition time of 1.8 ms.

As a result, we obtained novel GFID that renders injection system a reliable solution to be used in large-bore port fuel injection engines. The performance and emission of engine is a major area of future research.

ACKNOWLEDGMENT

This research was funded by the National Natural Science Foundation of China [51875326]; Shandong Provincial Natural Science Foundation, China [ZR2019MEE049]; National Natural Science Foundation of China [51805301];

National Key Research and Development Project, China [2017YFB0102004]; Shandong Provincial Agricultural Equipment Innovation Project, China [NJGG201505].

REFERENCES

- [1] Nakharutai N, Phetpradap P., "On the lowest unique bid auction with multiple bids", *Engineering Letters*, Vol. 23, No. 3, pp.125-131.2015.
- [2] Liccardo F, Strano S, Terzo M., "Optimal control using state-dependent riccati equation (SDRE) for a hydraulic actuator", *Lecture Notes in Engineering and Computer Science*, Vol. 3 LNECS, pp.2003-2007.2013.
- [3] Zhang J, Peng Z, Zhang L, Zhang Y., "A review on energy-regenerative suspension systems for vehicles", *Lecture Notes in Engineering and Computer Science*, Vol. 3 LNECS, pp.1889-1892.2013.
- [4] Liccardo F, Strano S, Terzo M., "Real-time nonlinear optimal control of a hydraulic actuator", *Engineering Letters*, Vol. 21, No. 4, pp.241-246.2013.
- [5] Chen G, Qian J, Zhang Z, Sun Z., "Multi-objective Improved Bat Algorithm for optimizing fuel cost, emission and active power loss in power system", *IAENG International Journal of Computer Science*, Vol. 46, No. 1, pp.118-133.2019.
- [6] Soberanis M. A. E., and Fernandez A. M., "A review on the technical adaptations for internal combustion engines to operate with gas/hydrogen mixtures", *Int J Hydrogen Energy*, Vol. 35, No. 21, pp. 12134-12140.2010.
- [7] Bircann R., Kazour Y., Dauer K., Fujita M., Wells A., Kabasin D. F., and Husted H., "Cold Performance Challenges with CNG PFI Injectors", *SAE paper*, No. 2013-01-0863. 2013.
- [8] Wang T, Chang S, and Liu L, "Influence of Injection Angle and Valve Opening Manner on Mixing Performance in a Large-Bore Port Fuel Injection Compressed Natural Gas-Fueled Engine", *J Eng Gas Turb Power*, Vol. 138, No. 12, pp.122804.2016.
- [9] Glasmachers H., Melbert J., and Koch A., "Sensorless Movement Control of Solenoid Fuel Injectors", *SAE paper*, No. 2006-01-0407.2013.
- [10] Liu L., and Chang S., "Motion Control of an Electromagnetic Valve Actuator Based on the Inverse System Method", *P Mech Eng D J Aut*, Vol. 226, No. 8, pp.85-93.2011.
- [11] Mercorelli P., "An Antisaturating Adaptive Preaction and a Slide Surface to Achieve Soft Landing Control for Electromagnetic Actuators", *IEEE/ASME Trans. Mech*, Vol. 17, No. 1, pp.76-85.2011.
- [12] Yang Y. P., Liu J., Ye D., Chen Y., and Lu P., "Multiobjective Optimal Design and Soft Landing Control of an Electromagnetic Valve Actuator for a Camless Engine", *IEEE/ASME Trans. Mech*, Vol. 18, No. 3, pp.963-972.2013.
- [13] Espinosa, A. G., and Ruiz, J. R. R., and Morera, X. A., "A Sensorless Method for Controlling the Closure of a Contactor," *IEEE Trans. Magn*, Vol. 43, No. 10, pp.3896-3903.2007.
- [14] Tsai J., Koch C. R., and Saif M., "Cycle Adaptive Feedforward Approach Controllers for an Electromagnetic Valve Actuator", *IEEE Trans. Contr. Syst. Tech*, Vol. 20, No. 3, pp.738-746.2012.
- [15] Ranft E. O., Schoor G., and Rand C. P., "Self-sensing for Electromagnetic Actuators. Part II: Position Estimation", *Sensors and Actuators A Physical*, Vol. 172, No. 2, pp.410-419.2011.
- [16] Dülk I., and Kováčsházy D., "A Sensorless Method for Detecting Spool Position in Solenoid Actuators", *Carpathian Journal of Electronic and Computer Engineering*, Vol. 6, No. 1, pp.36-43.2013.
- [17] Nagai S., Nozaki T., and Kawamura A., "Environmental Robust Position Control for Compact Solenoid Actuators by Sensorless Simultaneous Estimation of Position and Force", *IEEE Trans. Ind. Electron*, Vol. 63, No. 8, pp. 5078-5086.2016.
- [18] Sadighi A., "Adaptive-Neuro-Fuzzy-Based Sensorless Control of a Smart-Material Actuator", *IEEE/ASME Trans. Mech*, Vol. 16, No. 2, pp.371-379.2011.
- [19] Nagai S., Nozaki T., and Kawamura A., "Real-time Sensorless Estimation of Position and Force for Solenoid Actuators", *IEEJ Journal of Industry Applications*, Vol. 5, No. 2, pp.32-38.2016.
- [20] Mercorelli P., "An Adaptive and Optimized Switching Observer for Sensorless Control of an Electromagnetic Valve Actuator in Camless Internal Combustion Engines", *Asian J Cont*, Vol. 16, No. 4, pp.959-973.2014.
- [21] Mercorelli P., "A Hysteresis Hybrid Extended Kalman Filter as an Observer for Sensorless Valve Control in Camless Internal Combustion Engines", *IEEE Trans. Ind. Appl*, Vol. 8, No. 6, pp.1940-1949.2012.
- [22] Mercorelli P., "A Two-stage Augmented Extended Kalman Filter as an Observer for Sensorless Valve Control in Camless Internal Combustion Engines", *IEEE Trans. Ind. Electron*, Vol. 59, No. 11, pp.4236-4247.2015.
- [23] Vuoristo T., and Creep V., "Recovery and High Strain Rate Response of Soft Roll Cover Materials", *Mechanics of Materials*, Vol. 34, No. 8, pp.493-504.2002.
- [24] Tan C., Ge W., Fan X., Lu J., Li B., Sun B., "Bi-stable actuator measurement method based on voice coil motor", *Sensors Actuators A*, Vol.285, pp.59-66, 2019.